PHYSICAL REVIEW A VOLUME 11, NUMBER 6 JUNE 1975

Energy loss and straggling of 100–500-keV $_{90}$Th, $_{82}$Pb, $_{80}$Hg, and $_{64}$Gd in H_2

P. Hvelplund

Institute of Physics, University of Aarhus, DK-8000 Aarhus C, Denmark

(Received 25 November 1974)

Energy-loss distributions of $_{90}$Th, $_{82}$Pb, $_{80}$Hg, and $_{64}$Gd after passage through hydrogen are reported in the energy interval $100 < E < 500$ keV. The first three moments were extracted and compared with theoretical values of Lindhard *et al.* and reasonable agreement was obtained. Calculations of the energy-loss distributions were performed for the case where the projectiles lose their energy by elastic collisions with target atoms. Examples of calculated distributions are shown together with measured distributions.

INTRODUCTION

The present paper is part of a more extensive experimental investigation of energy loss and energy straggling suffered by keV ions penetrating gas targets.[1] The other parts of the work have been published previously.[2,3]

The energy loss of ions with a velocity $v < 0.1 \times v_0 Z_1^{2/3}$, where v_0 is the Bohr velocity and Z_1 the atomic number of penetrating ions, is due mainly to elastic collisions with target atoms. A theoretical treatment of energy loss and energy straggling in these so-called nuclear collisions was presented by Lindhard *et al.*[4] Rather few measurements of stopping cross sections exist in the region where nuclear stopping is the dominant mode of energy loss. Sidenius[5] measured stopping cross sections and energy straggling in hydrogen for various heavy ions $26 < Z_1 < 92$ in the 20–50-keV energy interval. Zahn,[6] Marx,[7] Poole *et al.*,[8] and Hancock *et al.*[9] determined the energy loss of α-recoil particles in carbon foils; Högberg[10] reported energy-loss measurements from which the nuclear stopping was extracted. Recently, Sidenius[11] has reported energy-loss measurements for light ions in methane.

When the projectile mass M_1 is of the same order or smaller than the mass of the target atom M_2, the distribution in nuclear energy loss may depend strongly on the angle between the initial beam and the direction of observation. In this respect, the situation is simpler for heavy projectiles and not-too-thin targets, and it was therefore decided to investigate nuclear stopping for heavy ions penetrating a hydrogen gas.

Energy loss of a charged particle in random matter is a statistical phenomenon in which the collisions responsible for the loss are independent events. Often only the average value of the resulting energy distribution is measured. However, in the following we shall investigate the distributions in more detail and make comparisons with theoretical predictions.

Measurements of the first three moments in the energy-loss distribution are performed on $_{90}$Th, $_{82}$Pb, $_{80}$Hg, and $_{64}$Gd in H_2 gas in the energy interval between 100 and 500 keV. In a few cases, the complete distribution is calculated as described below, and these theoretical distributions are compared with measurements.

THEORY

The slowing-down process has been described by Bohr,[12] who showed that the mean energy loss and the mean-square deviation of the energy distribution after passage through a target of thickness ΔR can be expressed as

$$\langle \Delta E \rangle = N \Delta R \int T \, d\sigma(T) . \tag{1}$$

and

$$\langle (\Delta E - \langle \Delta E \rangle)^2 \rangle = \Omega^2 = N \Delta R \int T^2 d\sigma(T) , \tag{2}$$

where $d\sigma(T)$ is the differential cross section for an energy transfer in the interval $(T, T + dT)$ and N is the number of atoms per unit volume. It is assumed that $d\sigma(T)$ is approximately constant on the pathlength ΔR, i.e., $\langle \Delta E \rangle \ll E_0$, where E_0 is the initial energy.

As shown by Bohr, the energy losses will be distributed according to a Gaussian,

$$W(\Delta E) = (2\pi\Omega^2)^{-1/2} \exp[-(\Delta E - \langle \Delta E \rangle)^2 / 2\Omega^2] , \tag{3}$$

provided $\Omega > T_m$, T_m being the maximum energy transfer in a single collision. The energy-loss distribution in Eq. (3) is fully characterized by the two parameters $\langle \Delta E \rangle$ and Ω. If the condition $\Omega > T_m$ is not fulfilled, one must have recourse to a more general method for obtaining the energy distribution. As described by Landau,[13] the general kinetic equation for the energy-loss distribution of particles having traversed a layer of

matter of thickness ΔR can be written in the following form,

$$\frac{\partial W(\Delta E, N\Delta R)}{\partial (N\Delta R)} = \int_{T=0}^{T=\infty} [W(\Delta E - T, N\Delta R) - W(\Delta E, N\Delta R)]\, d\sigma(T) . \quad (4)$$

Here it is also assumed that we are in the so-called "thin-absorber" approximation where $d\sigma(T)$ is independent of ΔE. The upper limit of the integration may be chosen as ∞ since $W(\Delta E, N\Delta R) = 0$, for $\Delta E < 0$ and $d\sigma(T) = 0$, for $T > T_m$.

Landau[13] solved Eq. (4) by making a Laplace transformation with respect to ΔE and obtained

$$W(\Delta E, N\Delta R) = \frac{1}{2\pi i} \int_{-i\infty+\sigma}^{i\infty+\sigma} dp \times \exp\left[p\Delta E - N\Delta R \int_0^\infty (1 - e^{-Tp})\, d\sigma(T)\right] . \quad (5)$$

The integration over p on a straight line parallel to the imaginary axis is to be performed for a positive value of σ.

Lindhard *et al.*[4] argue that the elastic interaction between two atoms can be derived from a potential,

$$V(r) = (Z_1 Z_2 e^2/r)\varphi_0(r/a) , \quad (6)$$

where φ_0 is the Fermi function belonging to an isolated atom and $a = 0.8853 a_0 (Z_1^{2/3} + Z_2^{2/3})^{-1/2}$. Here a_0 is the Bohr radius and Z_1 and Z_2 are the atomic numbers of the projectile and target, respectively. This type of potential is shown to lead to a differential cross section,

$$d\sigma = -\pi a^2 (dt/2t^{2/3}) f(t^{1/2}) , \quad (7)$$

where

$$t = TE \frac{M_2}{M_1} \left(\frac{2Z_1 Z_2 e^2}{a}\right)^{-2} , \quad (8)$$

E being the projectile energy and $f(t^{1/2})$ tabulated in Ref. 4.

Lindhard *et al.*[4] also consider other potentials, among which the Lenz-Jensen static potential will be used in the present calculations. Equation (6) is, however, still valid in this case, but f has to be derived for each potential used. For the present purpose, f has been approximated by the analytical expression,

$$f(x) = \tfrac{1}{2} x^{1/2} (0.48 + x^{3/3.2})^{-1.6} , \quad (9)$$

when the Lenz-Jensen potential is used. The values of $f(x)$ calculated from this expression agree to within 2% with those reported by Lindhard *et al.*[4]

On the basis of the differential cross section in Eq. (7), a reduced stopping cross section and straggling can be expressed in dimensionless units for energy, range, and mass, ϵ, ρ, and γ respectively, where

$$\epsilon = \frac{aM_2 E}{Z_1 Z_2 e^2 (M_1 + M_2)} , \quad (10)$$

$$\rho = \frac{4\pi a^2 M_1 M_2}{(M_1 + M_2)^2} NR , \quad (11)$$

and

$$\gamma = \frac{4M_1 M_2}{(M_1 + M_2)^2} . \quad (12)$$

The reduced stopping cross section is given by

$$s(\epsilon) = \frac{1}{2\epsilon} \int_0^{\epsilon^2} \frac{f(t^{1/2})}{t^{1/2}}\, dt , \quad (13)$$

and the straggling by

$$w(\epsilon) = \frac{1}{2\epsilon^2} \int_0^{\epsilon^2} t^{1/2} f(t^{1/2})\, dt . \quad (14)$$

$s(\epsilon)$ and $w(\epsilon)$ corresponding to the Thomas-Fermi screening function φ_0 are tabulated in Ref. 4. The connection between the measured values $\langle \Delta E \rangle / \Delta R$ and $\Omega^2/\Delta R$ and the corresponding reduced quantities is given by the relations

$$s(\epsilon) = \frac{\langle \Delta E \rangle}{\Delta R} \frac{\epsilon}{E} \frac{R}{\rho} \quad (15)$$

and

$$w(\epsilon) = \frac{\Omega^2}{\Delta R} \left(\frac{\epsilon}{E}\right)^2 \frac{R}{\rho} \frac{1}{\gamma} . \quad (16)$$

As can be easily shown, the third moment of the energy distribution can also be expressed as an integral over energy transfer in the following simple way,

$$\Sigma^3 = \langle (\Delta E - \langle \Delta E \rangle)^3 \rangle = N\Delta R \int T^3\, d\sigma , \quad (17)$$

or in dimensionless units,

$$a(\epsilon) = \frac{1}{2\epsilon^3} \int_0^{\epsilon^2} t^{3/2} f(t^{1/2})\, dt . \quad (18)$$

This reduced quantity is related to $\Sigma^3/\Delta R$ through the equation,

$$a(\epsilon) = \frac{\Sigma^3}{\Delta R} \left(\frac{\epsilon}{E}\right)^3 \frac{R}{\rho} \frac{1}{\gamma^2} . \quad (19)$$

With the cross section (7), we can solve expression (5) for the energy-loss distribution (see Appendix), and in dimensionless units we obtain

$$W(\Delta\epsilon, \rho) = \frac{1}{\pi} \int_0^\infty \exp[-(\rho/\gamma) A(y)] \times \cos[y\Delta\epsilon - (\rho/\gamma) C(y)]\, dy , \quad (20)$$

where

$$A(y)=2\int_0^{\epsilon}\sin^2\left(\frac{\gamma x^2}{2\epsilon}y\right)\frac{f(x)}{x^2}\,dx \tag{21}$$

and

$$C(y)=\int_0^{\epsilon}\sin\left(\frac{\gamma x^2}{\epsilon}y\right)\frac{f(x)}{x^2}\,dx\,. \tag{22}$$

Kessel'man[14] considered the same problem, including the effect of multiple scattering, and Vavilov,[15] Seltzer and Berger,[16] and Shulek *et al.*[17] solved Eq. (5) using the Rutherford-scattering cross section for collisions with the target electrons.

EXPERIMENTAL PROCEDURE AND EXTRACTION OF DATA

Since the details of the experimental procedure were presented in a previous paper,[2] only a brief description will be given here. The ions were produced in the Aarhus 600-keV heavy-ion accelerator and selected in a 75° sector magnet. After deflection, the ions passed through a 828 ±1 mm long differentially pumped target chamber (Fig. 1).

By means of an analyzing magnet, the energy distribution of the emerging ions was determined. Detector D counted neutrals and was used for normalization, and thus fluctuations in the beam current did not influence the measurements. The incident energy E_0 was also determined by means of the analyzing magnet with no gas in the target chamber. The energy resolution of the analyzing system was ~0.1%. The commercial supplier stated the purity of the H_2 gas to be 99.9994%.

The energy spectra obtained were analyzed in terms of moments. Let us first consider the simple situation in which the energy distribution is a Gaussian. In this case, $\langle\Delta E\rangle$ is the energy difference between the peak values of the energy distribution measured with and without gas in the target cell. Ω is given as $(1/2.36)\times$FWHM (full width at half-maximum) of the distribution measured with gas in the target cell. No correction was made for the width of the primary peak because it was less than 1% of the width of the energy distribution after penetration.

For asymmetric energy distributions, the moments $P_1=\langle\Delta E\rangle$, $P_2=\Omega^2$, $P_3=\Sigma^3$ were found from the following expression by numerical integration,

$$P_1=\frac{\int_0^{\infty}\Delta E\,W(\Delta E)\,d(\Delta E)}{\int_0^{\infty}W(\Delta E)\,d(\Delta E)}\,,$$

$$P_n=\frac{\int_0^{\infty}(\Delta E-\langle\Delta E\rangle)^n\,W(\Delta E)\,d(\Delta E)}{\int_0^{\infty}W(\Delta E)\,d(\Delta E)}\,,\quad n\geq 2\,. \tag{23}$$

The stopping cross section is given by $S=\langle\Delta E\rangle/N\Delta R$ at the energy $E=E_i-\frac{1}{2}\langle\Delta E\rangle$, and at the same energy, the straggling is given as $\Omega^2/N\Delta R$.

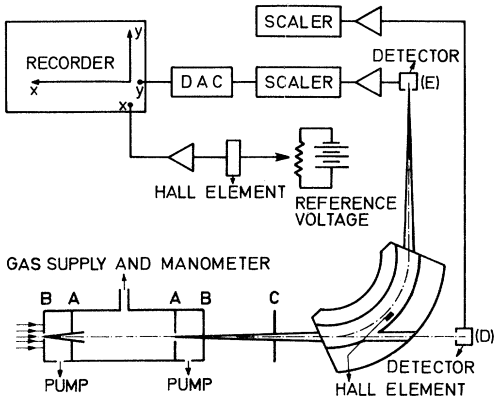

FIG. 1. Diagram of the apparatus.

The nonsystematic errors are ~3% in the gas-pressure measurements and ~1% in the temperature measurements. Systematic errors are due to uncertainties in target length (0.5%), in McLeod-gauge calibration (0.4%), in magnetic field (0.5%), and in energy (0.1%). The uncertainty is therefore estimated to be ~5% for S and ~10% for $\Omega^2/N\Delta R$.

DISCUSSION AND RESULTS

The results can conveniently be divided into two groups, one corresponding to $\Omega > T_m$ and one to $\Omega \lesssim T_m$.

For $\Omega > T_m$, the energy-loss distribution is expected to be Gaussian and experimentally it was found that whenever $\Omega \gtrsim 2T_m$, this is indeed the case.

In the experiment, only the central cone of the transmitted beam was energy analyzed. The acceptance angle was normally smaller than the root mean square of the angular distribution, but as shown by Sidenius,[5] the energy loss is independent of the acceptance angle as long as the energy distribution is symmetric (also see below).

Figure 2 compares the theoretically predicted stopping cross sections with the values measured here and with those obtained by Sidenius. The three theoretical curves represent nuclear stopping calculated from a Thomas-Fermi potential and from a Lenz-Jensen potential and the total stopping as the sum of Thomas-Fermi nuclear stopping and electronic stopping. The latter is found from the formula,

$$\frac{d\epsilon}{d\rho}=0.1\epsilon^{1/2}\,, \tag{24}$$

(see, e.g., Lindhard *et al.*[18]). It is noted that in the present ϵ range, the electronic contribution

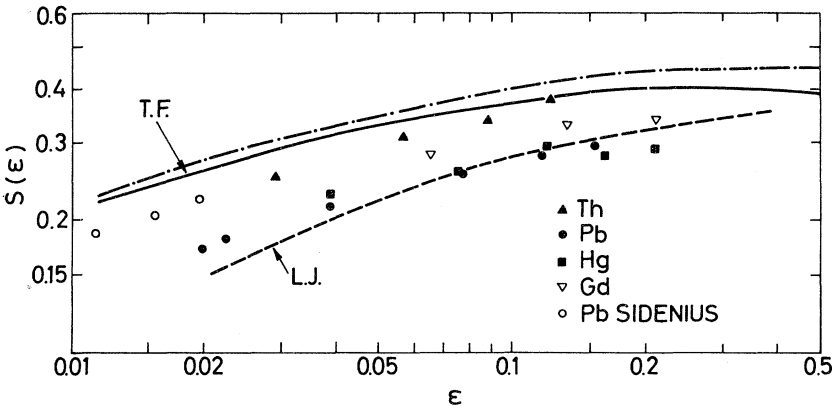

FIG. 2. Reduced stopping cross sections s as a function of ϵ. Fully drawn curve corresponds to the Thomas-Fermi potential, dashed curve to the Lenz-Jensen potential, and dash-dot curve to the sum of nuclear- (TF) and electronic-stopping cross section (see text). The points are experimental values.

to the total energy loss is estimated to amount to less than 10%. It is assumed that the hydrogen molecule acts as two independent hydrogen atoms, an assumption which seems justified by the facts that the collision time is $\sim 10^{-3}$ times a typical vibration time for a H_2 molecule and that the interaction potential is mainly determined by the heavy collision partner.

All of the experimental points fall from 10% to 30% below the theoretical curve for the total stopping cross section. Deviations of this order of magnitude between theory and experiment have also been found by others[6-10] for various projectile-target combinations. The results for Pb and Hg are seen to agree very well with the theoretical curve calculated from the Lenz-Jensen potential. At 60 keV, the present value for Pb is 25% lower than the one reported by Sidenius.[5] This rather large discrepancy has not yet been understood.

Any interaction potential of the form $V(r) = (Z_1 Z_2 e^2/r)\mu(r/a)$ leads to a universal function $s(\epsilon)$. Thus all of the experimental points should fit a single curve in a plot of $s(\epsilon)$ vs ϵ, irrespective of the projectile-target combination. Obviously this is not the case as the points scatter much more than the experimental errors. Besides a possible failure of the similarity approximation, the reason may stem from differences in the inelastic energy loss. Oscillations in the inelastic energy loss as a function of Z_1 have been observed by several authors, see, e.g., Ref. 19. It has been demonstrated that the amplitude in these oscillations increases with decreasing projectile velocity. It has further been found that the amplitude in these oscillations is ~50% of the theoretical value at velocities ~3 times as large as the present ones. It is therefore reasonable to assume that the large stopping-power value observed for Th is caused by a larger-than-average contribution from inelastic collisions.

Figure 3 shows the experimental straggling values together with the theoretical curves, based on the Lenz-Jensen and the Thomas-Fermi models of the atom. For comparison, also Sidenius's experimental values for Pb[5] are shown. It should be noted that the theoretical curves agree rather well with the general trend of the experimental data, and within the experimental uncertainty, the measured points lie on a single curve. This indicates that in the present energy range, the similarity may be a better approximation for the more violent collisions which dominate the energy straggling. This was to be expected since the similarity is exact in the limit of an unscreened Coulomb potential.

For $\Omega \lesssim T_m$, the problem is more complicated for two reasons. First, the energy distribution is no longer fully characterized by the two parameters $\langle \Delta E \rangle$ and Ω. Second, the energy distribution in the forward direction is not always the same as the distribution obtained when all of the transmitted particles are counted since ions suffering large energy losses are more likely to be scattered through large angles than are ions which have only experienced soft collisions.

However, if the angular distribution of the entire transmitted beam is well described by a Gaussian, the energy distribution is expected to be independent of the acceptance angle of the analyzing system. This is so since a Gaussian is obtained when the angle of emergence of a particle contains no information about the deflection experienced by the particle during penetration.

The mean-square deviation of the multiple-scattering distribution of ions emerging from a target is given by

$$\psi^2 = N \Delta R \int_0^{\varphi_m} \varphi^2 \, d\sigma \,, \tag{25}$$

where $d\sigma$ is the cross section for angular deflec-

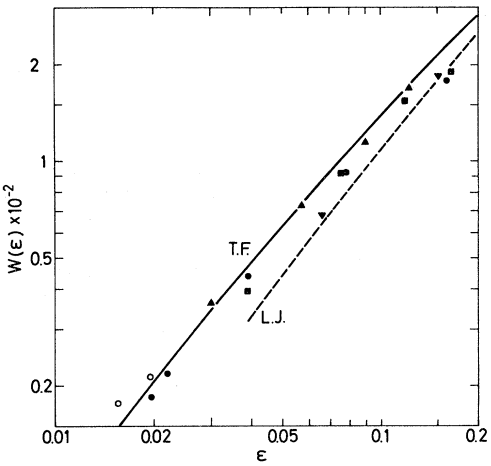

FIG. 3. Reduced energy straggling as a function of ϵ. The symbols are the same as those used in Fig. 2.

tion in the interval $(\varphi,\ \varphi+d\varphi)$ and φ_m is the maximum deflection in a single collision.

A Gaussian energy distribution is obtained for $\Omega > T_m$. Similarly, the deflection results in a Gaussian angular distribution for $\psi > \varphi_m$.

It can easily be shown[20] that the target thickness required to give a Gaussian angular distribution is smaller than that required for a Gaussian energy distribution. Thus, in an intermediate region of target thickness, the energy distribution is expected to be asymmetric but independent of the acceptance angle. In this region, a few measurements were performed, and Figs. 5 and 6

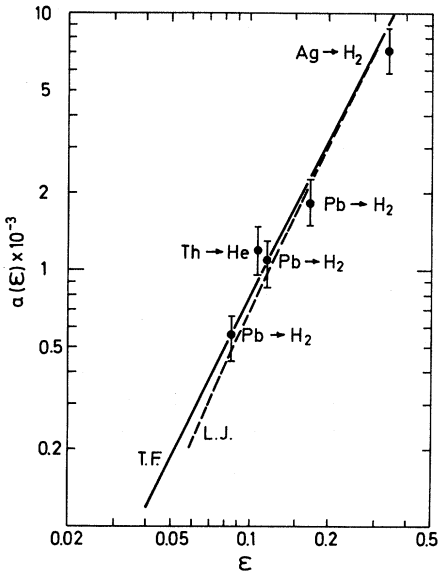

FIG. 4. Third moment in reduced units as a function of ϵ. Fully drawn curve corresponds to the Thomas-Fermi potential. Experimental values for Ag in H_2 and Th in He are also included.

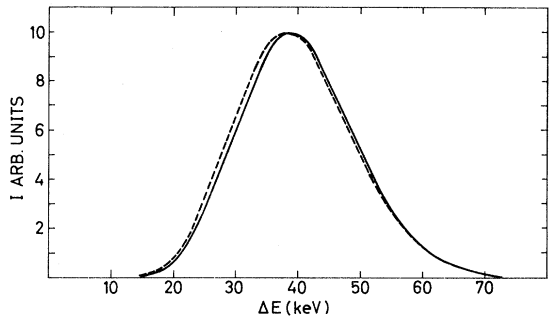

FIG. 5. Energy-loss distribution of 300-keV Pb ions in 4.51×10^{17} molecules/cm^2 hydrogen. Fully drawn curve is calculated from Eq. (20), using a Lenz-Jensen potential. Dashed curve is the measured distribution.

show that asymmetric energy distributions were indeed obtained. Stopping cross sections and straggling were evaluated from the curves, and the values agreed well with the corresponding values measured for thicker targets. This indicated that the energy distribution in the forward direction was the same as the energy distribution of the entire beam. In order to further check this assumption, the third moment was also extracted and compared with theory since higher moments will be more sensitive to the escape of ions having suffered violent collisions. Figure 4 shows that even the measured third moment agreed with theory within the experimental error. It should further be noted that the Lenz-Jensen and the Thomas-Fermi potentials lead to almost the same value of $a(\epsilon)$. The reason for this is that the higher moments are dominated by the more violent collisions for which the two potentials lead to approximately the same energy transfer.

Figures 5 and 6 also show a comparison of the measured distributions and the theoretical energy-loss distributions calculated from Eq. (20), using the Lenz-Jensen potential. The two examples correspond to cases in which the three first moments are known to agree nicely with theory, and we ob-

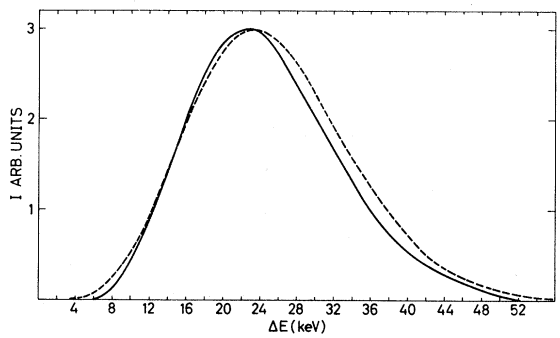

FIG. 6. Energy-loss distribution of 400-keV Pb ions in 5.40×10^{17} molecules/cm^2 hydrogen (cf. Fig. 5).

serve that under these circumstances, the Lenz-Jensen potential gives a good account of the full energy-loss distribution.

ACKNOWLEDGMENTS

I am much indebted to J. U. Andersen, E. Bonderup, and J. Lindhard for help received through numerous discussions. I am also grateful to P. Sigmund for encouraging me to publish these results and for his reading the manuscript prior to publication. My thanks are also due to the technical staff at the accelerator.

APPENDIX

Here, the calculation of the energy distribution $W(\Delta\epsilon)$ is described. Equation (5) can be written in the form

$$W(\Delta E, N\Delta R)=\frac{1}{2\pi i}\int_{-i\infty+\sigma}^{i\infty+\sigma} e^{I}\,dp, \tag{A1}$$

where

$$I=p\Delta E - N\Delta R\int_0^{T_m}(1-e^{-Tp})d\sigma . \tag{A2}$$

By means of the equations,

$$T=T_m t/\epsilon^2, \tag{A3}$$

$$N\Delta R=\frac{\rho E}{\pi a^2 T_m}, \tag{A4}$$

$$p_1=pE/\epsilon, \tag{A5}$$

and the cross section (6), Eq. (A2) can be written as

$$I=P_1\Delta\epsilon-\frac{\rho}{\gamma}\int_0^{\epsilon^2}(1-e^{(\gamma t/\epsilon)p_1})\frac{f(t^{1/2})}{2t^{3/2}}\,dt . \tag{A6}$$

Using the definition $p_1=p_0+iy$ and performing the integration along the imaginary axis, the following formula is obtained with $x=t^{1/2}$,

$$W(\Delta\epsilon,\rho)=\frac{1}{2\pi}\int_{-\infty}^{\infty}\exp\left\{iy\Delta\epsilon-\frac{\rho}{\gamma}\int_0^{\epsilon}\left[1-\exp\left(-\frac{\gamma x^2}{\epsilon}iy\right)\frac{f(x)}{x^2}\right]dx\right\}dy, \tag{A7}$$

or, as the imaginary part is zero,

$$W(\Delta\epsilon,\rho)=\frac{1}{2\pi}\int_{-\infty}^{\infty}\exp\left\{-\frac{\rho}{\gamma}\int_0^{\epsilon}\left[1-\cos\left(\frac{\gamma x^2}{\epsilon}y\right)\right]\frac{f(x)}{x^2}\,dx\right\}\cos\left[y\Delta\epsilon-\frac{\rho}{\gamma}\int_0^{\epsilon}\sin\left(\frac{\gamma x^2}{\epsilon}y\right)\frac{f(x)}{x^2}\,dx\right]dy, \tag{A8}$$

or

$$W(\Delta\epsilon,\rho)=\frac{1}{\pi}\int_0^{\infty}\exp\left(-\frac{\rho}{\gamma}A(y)\right)\cos[y\Delta\epsilon-(\rho/\gamma)C(y)]\,dy, \tag{A9}$$

where

$$A(y)=2\int_0^{\epsilon}\sin^2\left(\frac{\gamma x^2}{2\epsilon}y\right)\frac{f(x)}{x^2}\,dx \tag{A10}$$

and

$$C(y)=\int_0^{\epsilon}\sin\left(\frac{\gamma x^2}{\epsilon}y\right)\frac{f(x)}{x^2}\,dx . \tag{A11}$$

[1]P. Hvelplund, thesis (University of Aarhus, 1968) (unpublished).

[2]P. Hvelplund, K. Dan. Vidensk. Selsk. Mat.-Fys. Medd. 38, No. 4 (1971).

[3]E. Bonderup and P. Hvelplund, Phys. Rev. A 4, 562 (1971).

[4]J. Lindhard, V. Nielsen, and M. Scharff, K. Dan. Vidensk. Selsk. Mat.-Fys. Medd. 36, No. 10 (1968).

[5]G. Sidenius, *Proceedings of the Atomic Collisions Conference, London, 1963,* edited by M. R. C. McDowell (North-Holland, Amsterdam, 1963), p. 709.

[6]P. Zahn, Z. Phys. 172, 85 (1963).

[7]D. Marx, Z. Phys. 195, 26 (1966).

[8]D. H. Poole, A. G. Warner, R. Hancock, and R. L. Woolley, J. Phys. D 1, 309 (1968).

[9]R. Hancock, A. G. Warner, and R. Woolley, J. Phys. D 2, 991 (1969).

[10]G. Högberg, Phys. Status Solidi B 48, 829 (1971).

[11]G. Sidenius, K. Dan. Vidensk. Selsk. Mat.-Fys. Medd. 39, No. 4 (1974).

[12]N. Bohr, K. Dan. Vidensk. Selsk. Mat.-Fys. Medd. 18, No. 8 (1948).

[13]L. Landau, J. Phys. USSR 8, 201 (1944).

[14]V. S. Kessel'man, Zh. Eksp. Teor. Fiz. 59, 834 (1970) [Sov. Phys.—JETP 32, 456 (1971)].

[15]P. V. Vavilov, Zh. Eskp. Teor. Fiz. 32, 920 (1957) [Sov.

Phys.—JETP 5, 749 (1957)].
[16]S. Seltzer and M. J. Berger, Nat'l. Acad. Sci.-Natl. Res. Counc. Publ. 1133, 187 (1964).
[17]P. Shulek, B. M. Golovin, L. A. Kulyukina, S. V. Medved, and P. Pavlovich, Yad. Fiz. 4, 564 (1966) [Sov. J. Nucl. Phys. 4, 400 (1967)].
[18]J. Lindhard, M. Scharff, and H. E. Schiøtt, K. Dan. Vidensk. Selsk. Mat.-Fys. Medd. 33, No. 14 (1963).
[19]P. Hvelplund and B. Fastrup, Phys. Rev. 165, 408 (1968).
[20]B. Fastrup, P. Hvelplund, and C. A. Sautter, K. Dan. Vidensk. Selsk. Mat.-Fys. Medd. 35, No. 10 (1966).